THE ASTROPHYSICAL JOURNAL, 283:842–847, 1984 August 15


# SPECTRA FROM PAIR-EQUILIBRIUM PLASMAS

ANDRZEJ A. ZDZIARSKI[1]
Harvard-Smithsonian Center for Astrophysics, and Max-Planck-Institut für Physik und Astrophysik
*Received 1984 January 16; accepted 1984 February 29*

## ABSTRACT

Spectra from relativistic Maxwellian plasmas without magnetic fields or external photon sources and in pair equilibrium are presented. Photon emission by bremsstrahlung and pair annihilation processes, multiple Compton scatterings, and photon absorption by free-free and photon-photon pair production processes are modeled numerically using the Monte Carlo technique. Optical depth effects and equilibrium effects are solved for self-consistency by iteration. Pair annihilation features are found to be absent in all spectra from pair-equilibrium plasmas. Luminosities and radii typical for active galactic nuclei, $L \approx 10^{44}$ ergs s$^{-1}$ at $R \approx 10^{14}$ cm, correspond to models with temperature of $kT \approx 0.5 m_e c^2$ and the Thomson thickness $\tau_T \equiv (n_+ + n_-)\sigma_T R \approx 4$, where $m_e$ is the electron mass, $\sigma_T$ is the Thomson cross section, and $n_+$ and $n_-$ are the positron and electron densities, respectively. The resultant flat spectra differ, however, from typical active galactic nuclear spectra with a mean X-ray spectral index of $\sim 0.7$.

*Subject headings:* galaxies: nuclei — plasmas — radiation mechanisms — relativity — X-rays: sources

## I. INTRODUCTION

Relativistic plasmas in pair equilibrium have recently been a subject of increasing interest. The condition that pair production in a plasma cloud is balanced by pair annihilation leads to a relation connecting the positron density $n_+$, the temperature $T$, the luminosity $L$, and radius $R$ (Lightman 1982; Svensson 1982, 1984; Stepney 1983*a*). In particular, $n_+/N$ and $T$ can be expressed as single-valued functions of $L/R$ and $\tau_N$. Here $\tau_N \equiv N\sigma_T R$, $\sigma_T$ is the Thomson cross section, and $N$ is the density of ionization electrons. Futhermore, for a plasma with $\tau_T \gtrsim 1$ the time scale for photon escape is of the order of or longer than the time scale to establish pair equilibrium. Here $\tau_T$ is the Thomson scattering depth $\tau_T \equiv (n_+ + n_-)\sigma_T R$ and $n_-$ is the electron density. Thus, many steady cosmic X-ray and $\gamma$-ray sources are probably in pair equilibrium.

Previous work on pair equilibrium was either constrained to ultrarelativistic temperatures (Lightman 1982), or to cases with $dT/dL > 0$ (Stepney 1983*a*) or neglected Comptonization (Svensson 1982). On the contrary, the Monte Carlo method adopted in this work, originally developed by Pozdnyakov, Sobol', and Sunyaev (1977), can be used at any temperature and any Thomson thickness smaller than $\sim 10$. This method gives also detailed spectra of the emerging radiation as well as the radiation field inside the plasma cloud.

After our numerical calculations were completed, we received a preprint by Svensson (1984), in which he treated mildly relativistic Comptonization using an analytical approach. The relations between $T$, $L$, $R$, and $n_+/N$ obtained in that paper are in qualitative agreement with those presented here.

## II. NUMERICAL MODEL OF A RELATIVISTIC PLASMA CLOUD

A model of a spherical plasma cloud is described by the following parameters:

a) The dimensionless temperature $T_* \equiv kT/m_e c^2$;

b) The dimensionless optical thickness due to ionization electrons $\tau_N$;

c) The dimensionless Thomson thickness $\tau_T$;

d) The radius $R$.

The dimensional parameter $R$ enters only weakly, through the dependence of the low-energy spectrum on free-free absorption. The condition of pair equilibrium introduces a relation between the remaining three parameters. The Maxwellian electrons and positrons, which are assumed to have uniform spatial distributions, produce photons in the bremsstrahlung and pair annihilation processes. For the $e^{\pm}e^{\pm}$, $e^+e^-$, and $e^{\pm}p$ bremsstrahlung spectrum formulae see, e.g., Svensson (1982), Stepney and Guilbert (1983), and references in those papers. For the annihilation spectrum, the fitting formula of Zdziarski (1980) has been used.

In order to model multiple photon scatterings, the Monte Carlo method similar to that of Pozdnyakov, Sobol', and Sunyaev (1977) is used. In this method, the paths of individual photons are followed. Originally, in the Pozdnyakov *et al.* paper the probability of a scattering was assumed not to depend on the scattering angle. As discussed by Lorentz (1981) and Górecki and Wilczewski (1984), this assumption leads to an additional steepening of the optically thick spectra. In this paper the correct scattering probability was used.

Concurrently to scatterings there occurs a photon absorption due to either the inverse bremsstrahlung process at the low-energy end of a spectrum (see eqs. [4] and [5]) or the photon-photon pair production process at the high energy end (see below).

As the paths of individual photons are followed during the calculations, detailed radiation field inside the cloud can be determined as well as the emerging spectra. In the actual calculations, the radiation fields at five different optical depths below the surface of a cloud are determined. This enables us to calculate the rates of the pair production in photon-photon ($\gamma\gamma$), photon-positron or electron ($\gamma e^{\pm}$), and photon-photon ($\gamma p$) collisions and opacity due to the $\gamma\gamma$ process; $\gamma e^{\pm}$ and $\gamma p$ opacities and the rates of the $e^{\pm}e^{\pm}$ and $e^{\pm}p$ pair production and $e^+e^-$ pair annihilation can be found from the electron and positron distributions alone. For a review of the pair pro-

[1] On leave from N. Copernicus Astronomical Center, Bartycka 18, 00-716 Warsaw, Poland.

duction and pair annihilation rate formulae see, e.g., Svensson (1982, 1984). In order to avoid multidimensional integrations over photon angular distributions in the computations of the $\gamma\gamma$ pair production process, the radiation field inside the cloud was assumed to be isotropic. In such cases the optical thickness to the photon-photon pair production processes $\tau^{\gamma\gamma}$ reduces to a sum of one-dimensional integrals (see Gould and Schréder 1967; Brown, Mikaelian, and Gould 1973 for corrections).

The ratio of the total pair production rate $R_+$ and the pair annihilation rate $R_-$ tells us if the plasma is in pair equilibrium. Equilibrium solutions for which $R_+ = R_-$ are found by two iteration methods. First, the parameters (*a*)–(*d*) for which the cloud is in pair equilibrium can be found iteratively, e.g., by changing $\tau_T$ in consecutive models keeping other parameters constant. Second, if the optical thickness to the $\gamma\gamma$ pair production processes exceeds unity at an energy $x \equiv h\nu/m_e c^2$, a substantial part of photons with energy $x$ will be absorbed in $\gamma\gamma$ collisions before escape. This would cause a decrease in the radiation intensity $I_x$, which would, in turn, decrease the optical thickness $\tau^{\gamma\gamma}(x_1)$ at energies $x_1 > 1/x$. To account for nonlinearity of the process in the cases when $\tau^{\gamma\gamma}(x) \gtrsim 1$ at such $x$ that $I_x$ is still high, the following iteration method has been used:

1. In the first step the nonabsorbed radiation field $I_x^1[\alpha_x^0 \equiv 0]$ and opacity due to this field $\alpha_x^1[I_x^1]$ are calculated (see eqs. [9]–[12] of Gould and Schréder 1967).
2. The new absorbed field $I_x^2[\alpha_x^1]$ and its opacity $\alpha_x^2[I_x^2]$ are calculated.
3. In this step a mean opacity, usually $\langle\alpha_x\rangle \equiv (\alpha_x^1 + \alpha_x^2)/2$ is used to calculate $I_x^3[\langle\alpha_x\rangle]$ and $\alpha_x^3[I_x^3]$. The quantities $I_x^i$ and $\alpha_x^i$, $i = 1,2,3$, fulfill the relations $I_x^1 \geq I_x^3 \geq I_x^2$ and $\alpha_x^1 \geq \alpha_x^3 \geq \alpha_x^2$.
4. In most cases $I_x^3$ was already consistent with $\alpha_x^3$; i.e.,

$$I_x^4[\alpha_x^3[I_x^3]] \approx I_x^3 . \tag{1}$$

If this condition is not fulfilled, further iteration is carried out. In the above expressions brackets denote integral dependences. We find out that pair absorption substantially changes spectra and luminosities for optically thick plasmas with $n_+ \gg N$ and $T_* \lesssim 1$ (see Figs. 2*a*, 2*b*).

We point out that the Monte Carlo method can be used in principle to calculate spectra from any plasma, whether in equilibrium or not, provided only the pair density does not change substantially during the time a photon needs to escape; that is,

$$1 \gg \frac{t^{\rm esc}}{t^{\rm pair}} \approx \begin{cases} \dfrac{3}{16}\left(\tau_T + \dfrac{\tau_T^2}{2}\right)|r-1|, & T_* \ll 1, \\ \dfrac{3}{32}\left(\tau_T + \dfrac{\tau_T^2}{2}\right)|r-1|\dfrac{\ln T_*}{T_*^2}, & T_* \gg 1. \end{cases} \tag{2}$$

Here $t^{\rm esc} = R(1 + \tau_T/2)/c$, $t^{\rm pair} = n_+/|dn_+/dt|$, and $r = R_+/R_-$. All the plasmas considered in this paper are in pair equilibrium ($r = 1$) and, of course, satisfy equation (2).

## III. PLASMA IN PAIR EQUILIBRIUM: SPECTRA AND PARAMETERS

The ratio of the pair production and pair annihilation processes depends on all four parameters (*a*)–(*d*) defined in § II. Dependence on the radius, however, is only through the frequency $x_0$ below which emitted photons are mostly absorbed in the free-free process rather than scattered up in energy. The mean energy amplification in a single scattering can be approximated as $A \approx 1 + 4T_* + 16T_*^2$ (Svensson 1984). The mean number of scatterings in a uniform spherical cloud with $\tau_T \gg 1$ is $\tau_T^2/5$ (Sunyaev and Titarchuk 1980) and $\sim\tau_T$ for $\tau_T \ll 1$. Thus, the condition that photons scattered up from the frequency $x_0$ do not affect either the luminosity or the pair production rate can be written approximately as

$$x_0 A^{(\tau_T^2/5 + \tau_T)} \ll \frac{T_*}{T_*^2 + 1}, \tag{3}$$

where for the right-hand side it follows from the results that most of the luminosity in Comptonized bremsstrahlung-annihilation spectra is at photon energies $x \approx T_*$ and the threshold energy for pair production is $x \approx 1/T_*$. Since for mildly relativistic plasmas, $A \gtrsim 2$, $x_0$ is determined by

$$R\alpha_{\rm ff}(x_0) = \max(1, \tau_T), \tag{4}$$

and

$$x_0 \approx 4 \times 10^{-11} \min(\tau_T, \tau_T^{1/2}) \left[\frac{10^{14}\ {\rm cm}}{RT_*} \frac{\ln(T_*/x_0)}{30}\right]^{1/2}, \tag{5}$$

(see Lightman and Band 1981). When equation (3) is satisfied, the frequency $x_0$ becomes unimportant, and the radius $R$ no longer enters by itself as a determining parameter. In this case, $L \propto R$, and then it is convenient to replace $L$ by the dimensionless quantity $l \equiv L/L_0$, where $L_0 \equiv m_e c^3 R/\sigma_T = 3.70 \times 10^{42}$ $(R/10^{14}\ {\rm cm})$ ergs s$^{-1}$.

Figure 1 presents dependences of $\tau_T$ and $T_*$ on $l$ for three different values of $\tau_N$ equal to $10^{-3}$, 1, and $10^{1/2} = 3.16$. As found by Lightman (1982) and Svensson (1982), the dependence $T(L)$ is not monotonic; the temperature reaches a maximum value $T^{\rm max}(L)$ and then decreases with increasing luminosity. For $\tau_N \to 0$, $T_*^{\rm max}$ is equal to $\sim 25$. A plasma with $dT/dL < 0$ is isothermally unstable. It is stable, however, if the heating rate rather than the temperature is kept constant. In the cases when $(n_+ + n_-) \gg N$, $\tau_T \gg \tau_N$, and the thickness $\tau_N$ no longer enters as a determining parameter. For $\tau_N \lesssim 3.16$, the $T_*(l)$ and $\tau_T(l)$ functions become independent of $\tau_N$ at $l \gtrsim 30$ (see Fig. 1).

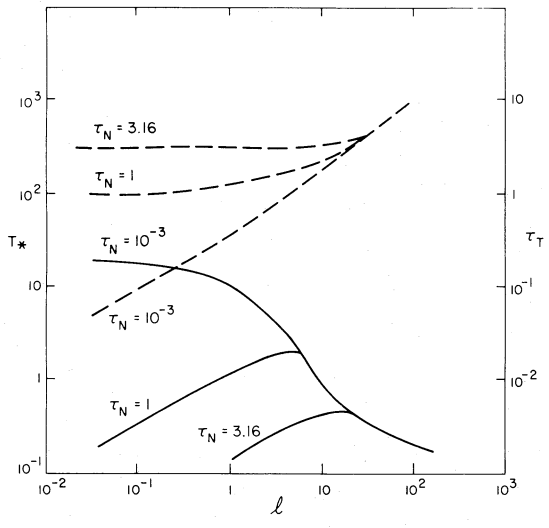


FIG. 1.—Temperature $T_*$ (*solid curves*) and the Thomson thickness $\tau_T$ (*dashed curves*) of plasmas in pair equilibrium as functions of the luminosity for three different $\tau_N$. The luminosity $l \equiv L/L_0$ is given in terms of $L_0 \equiv m_e c^3 R/\sigma_T = 3.70 \times 10^{42}(R/10^{14}\ {\rm cm})$ ergs s$^{-1}$. For $l \gtrsim 30$, all the shown functions become independent of $\tau_N$.

Figures 2*a*–2*e* present some typical spectra from plasmas in pair equilibrium. Characteristically, all the presented spectra are flat in the X-ray region, as would be expected from a bremsstrahlung emission process. As a typical active galactic nuclei (AGN) spectral index in that region is close to 0.7 (Halpern 1982; Rotschild *et al.* 1983), this indicates the importance of some other processes in AGN radiation production mechanisms. The spectra in Figures 2*a*–2*d* have been calculated for $\tau_N = 10^{-3}$ in the region where $dT/dL < 0$ (high pair density solutions). The spectrum in Figure 2*e* corresponds to the case with $\tau_N = 3.16$ and $dT/dL > 0$ (low pair density). In no spectra emergent from pair-equilibrium plasmas is an annihilation feature visible. At $T_* \lesssim 1$ an equilibrium plasma cloud either has negligible pair density or is optically thick, where any annihilation feature is smeared over by Compton scatterings (see Figs. 2*a*–2*e*). On the other hand, at $T_* \gtrsim 1$, where

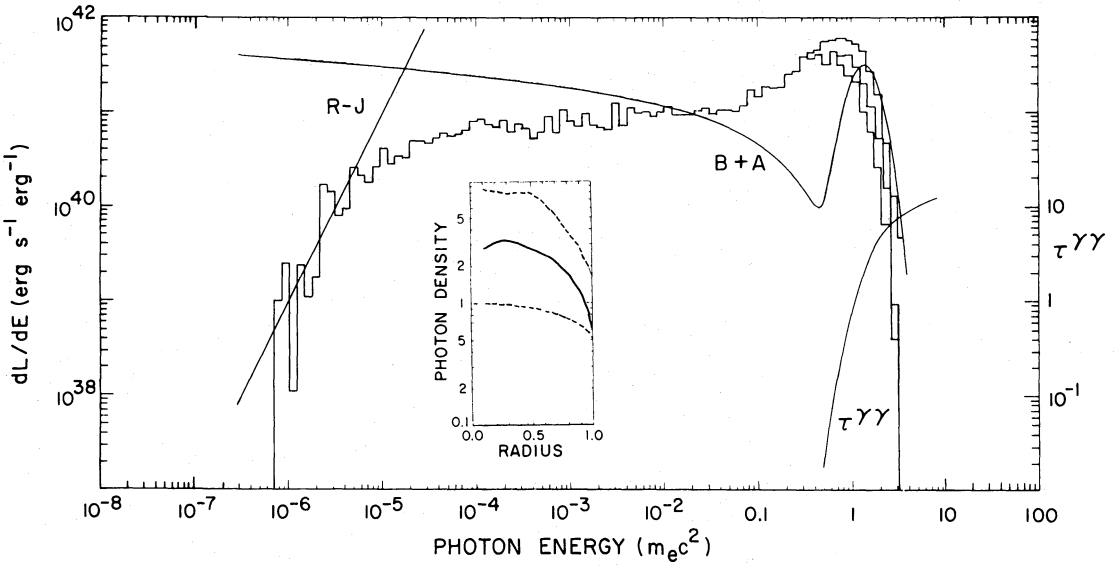


FIG. 2*a*

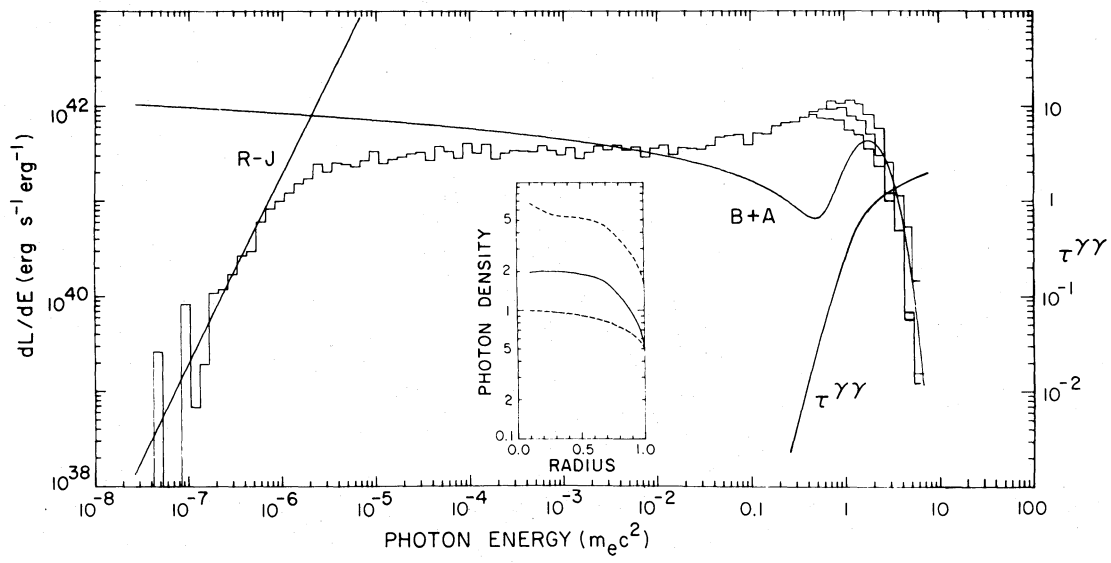


FIG. 2*b*

FIG. 2.—Energy spectra $dL/dE$ (ergs s$^{-1}$ ergs$^{-1}$) from pair-equilibrium plasmas for various temperatures $T_*$ and scattering thicknesses $\tau_N$ and $\tau_T$ (we remind the reader, $m_e c^2 = 0.82 \times 10^{-6}$ ergs). The luminosity $dL/dE$ is roughly proportional to the radius $R$ (see § III). Solid curves denoted B + A are the optically thin bremsstrahlung and pair annihilation spectra, those denoted R-J are the Rayleigh-Jeans spectra. Histograms resulting from the Monte Carlo calculations include both Comptonization and absorption effects. In (*a*)–(*b*), the iterative method of computing of pair absorption is demonstrated by the upper, medium, and lower histograms, corresponding to the $I_x^1$, $I_x^3$, and $I_x^2$ radiation fields, respectively (see § II). Curves denoted $\tau^{\gamma\gamma}$ in (*a*)–(*c*) are the optical thicknesses due to pair absorption (*right scale*). Insets in (*a*)–(*b*) show photon densities as functions of the radius (see § III). Plasma parameters are (*a*) $T_* = 0.25$, $\tau_N = 10^{-3}$, $\tau_T = 8$, the radius $R = 1.5 \times 10^5$ cm, the dimensionless luminosity $l = 72$, the energy amplification factor $\alpha = 1.3$, the ratio of the pair production rates in $\gamma\gamma$ and $\gamma e^{\pm}$ collisions $R_{\gamma\gamma}/R_{\gamma e} = 2.2 \times 10^4$; (*b*) $T_* = 0.5$, $\tau_N = 10^{-3}$, $\tau_T = 4$, $R = 1.5 \times 10^5$ cm, $l = 27$, $\alpha = 1.8$, $R_{\gamma\gamma}/R_{\gamma e} = 820$; (*c*) $T_* = 1$, $\tau_N = 10^{-3}$, $\tau_T = 2.2$, $R = 1.5 \times 10^5$ cm, $l = 12$, $\alpha = 2.8$, $R_{\gamma\gamma}/R_{\gamma e} = 70$; (*d*) $T_* = 3.16$, $\tau_N = 10^{-3}$, $\tau_T = 1$, $R = 1.5 \times 10^6$ cm, $l = 4.5$, $\alpha = 3.0$, $R_{\gamma\gamma}/R_{\gamma e} = 7.6$; (*e*) $T_* = 0.3$, $\tau_N = 3.16$, $\tau_T = 3.18$, $R = 4.8 \times 10^8$ cm, $l = 4.2$, $\alpha = 9.2$.

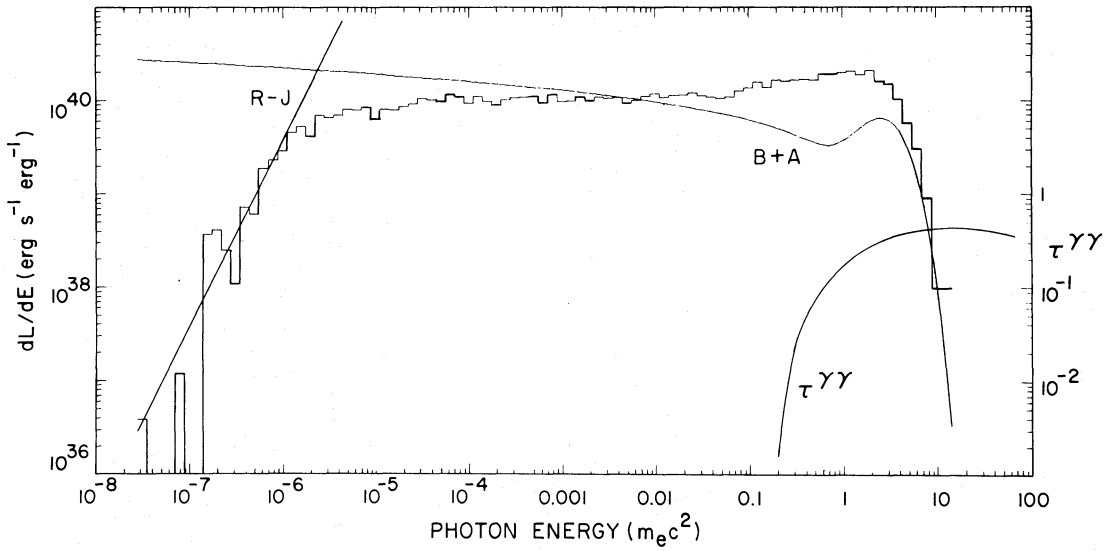


FIG. 2c

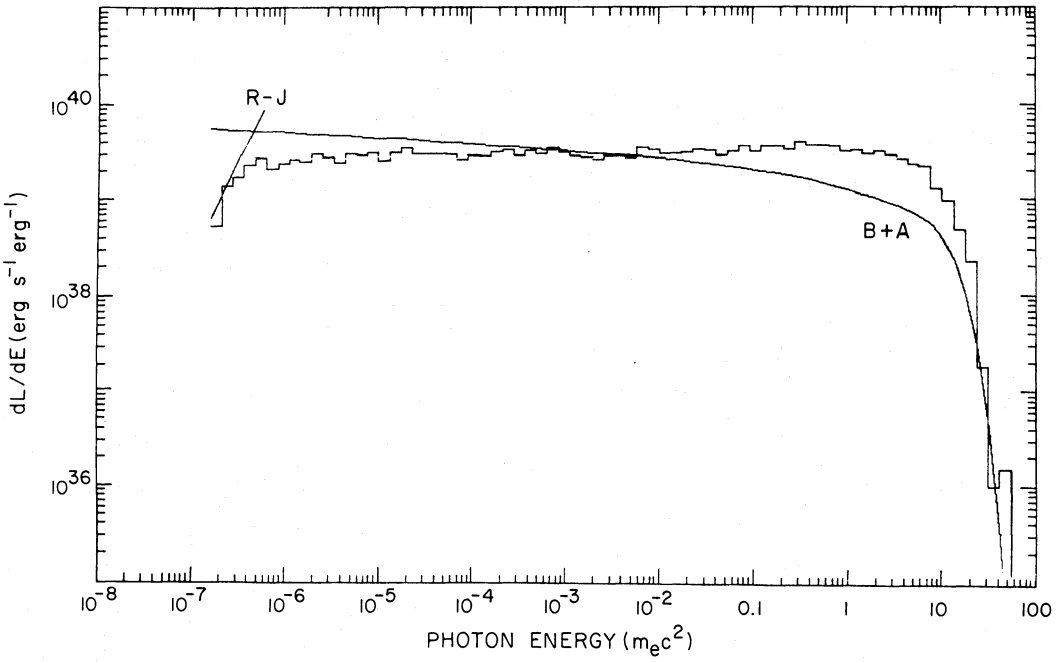


FIG. 2d

an optically thin, high pair density plasma can be in pair equilibrium, annihilation photons form a very broad feature which is indistinguishable when superposed on the bremsstrahlung spectrum (Fig. 2*d*). The spectra shown in Figures 2*a*–2*b* have intensity peaks at $x \sim 3T_*$, which are, however, much broader than the corresponding Wien spectra at the same temperatures. For the spectra in Figures 2*a*–2*b*, the effect of pair absorption is also shown. The upper histograms in the high-energy tails of the spectra have been calculated neglecting pair absorption ($I_x^1$ in the notation of § II), whereas the lower ones correspond to $I_x^2$, and the medium ones are the self-consistent spectra $I_x^3$. The optical thicknesses $\tau^{\gamma\gamma}$ are also plotted in Figures 2*a*–2*c*. As seen in Figures 2*a*–2*b*, pair absorption tends to decrease the contribution to the spectrum from the scattered annihilation photons. The insets in Figures 2*a*–2*b* present photon densities as functions of the radius for (i) all photons present in the cloud (*solid curves*) and normalized to the density in a cloud of vanishing Thomson thickness (*lower dashed curves*); and (ii) for photons above the threshold for $\gamma\gamma$ pair production (*upper dashed curves*) normalized to the above-threshold density of a cloud of vanishing Thomson thickness. The densities (i) are substantially lower than those predicted by the relation $n_\gamma(\tau_T \gtrsim 1) = n_\gamma(0)\tau_T$. This is because the mean Thomson depth at which a photon is produced is less than $\tau_T$ for a sphere and because the Thomson cross section substantially decreases at relativistic energies. Furthermore, a correction for free-free absorption, which has not been made, would increase the total photon density (*solid curves*) by $\sim 30\%$. The spectra in Figures 2*c*–2*e* are characterized by zero spectral indices regardless of temperature and the optical thickness $\tau_T$.

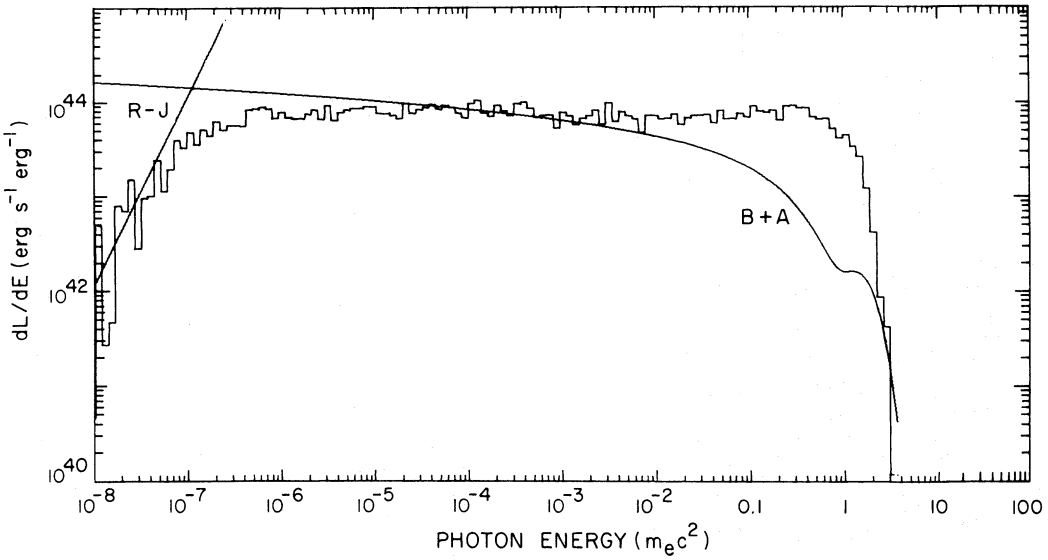


FIG. 2e

For all the spectra presented in Figure 2, $\gamma\gamma$ is the dominant pair production process; i.e. the ratio of rates of $\gamma\gamma$ to $\gamma e^{\pm}$ pair production, $R_{\gamma\gamma}/R_{\gamma e}$, is much greater than unity. For $\tau_N \ll 1$ and $dT/dL < 0$, $R_{\gamma e}$ becomes greater than $R_{\gamma\gamma}$ at $10 < T_* < 20$, while at $20 < T_* < T_*^{\max} \approx 25$ particle-particle collisions dominate (the limiting values of $T_*$ equal to 10 and 20 obtained by us are the same as those shown in Fig. 7 by Svensson 1982).

In the cases with high $\tau_T$, bremsstrahlung photons undergo a high amplification of energy in multiple photon scatterings. However, in the cases with $n_+ \gg N$ and $T_* \lesssim 1$, the bulk of the emitted energy is in annihilation photons, which lose energy in Compton scatterings. Consequently, the net energy amplification for pair-dominated plasmas with $T_* \lesssim 1$ is small, $l \approx (1.3 \div 2.8)(l_B + l_A)$, where $l_B$ and $l_A$ are the dimensionless bremsstrahlung and pair annihilation luminosities, respectively. Specifically, for $T_* \ll 1$ and $n_+ \gg N$, $l_B \ll l_A = (\pi/2)\tau_T^2$.

Figure 3 shows the time scale for cooling $t_*^{\rm cool}$, and the electron-electron energy exchange time $t_*^{ee}$ expressed in units of the Thomson time $t_T \equiv [(n_+ + n_-)\sigma_T c]^{-1}$ and as functions of the luminosity $l$. For the latter time scale, the results of Stepney (1983*b*) have been used. The cooling time $t_*^{\rm cool}$ is shorter than $t_*^{ee}$ for $T_* \gtrsim 5$, as found by Stepney (1983*b*) and Gould (1982); Comptonization does not change this result. The quantity $t_*^{\rm cool}$ was found within a factor of $\sim 1.5$ to be a unique function of the luminosity $l$ independently of $\tau_N$ as far as $l > 0.1$. For $l \gtrsim 100 (\tau_T \gtrsim 10)$, the cooling time becomes shorter than the Thomson time; i.e., $t_*^{\rm cool} < 1$.

## IV. CONCLUSIONS

In this paper a numerical model of relativistic non-magnetized plasma with uniform temperature and electron density distributions was considered, and spectra from plasmas in pair equilibrium were studied. The temperature range $T_* \gtrsim 0.2$ was considered. The spectra from low pair density plasmas in pair equilibrium vary from uncomptonized bremsstrahlung spectra at $\tau_N \ll 1$ to Comptonized bremsstrahlung spectra at $\tau_N \gtrsim 1$ such as shown in Figure 2*e* (see Zdziarski 1984). For high pair density plasmas the spectra are flat for $T_* \gtrsim 1$ (Figs. 2*c*–2*d*) and have broad intensity peaks at $x \approx 3T_*$ for $T_* \lesssim 1$ (Figs. 2*a*–2*b*). In the latter region the total luminosity is approximately twice the annihilation luminosity. No spectra, however, reveal any annihilation feature. Pair absorption modifies high-energy tails of optically thick high pair density spectra, tending to reduce the contribution from the scattered annihilation photons. All spectra are flat in the X-ray region, in contradiction to observed AGN spectra, with a mean spectral index of $\sim 0.7$.

The cooling time, the *e-e* relaxation time, and the Thomson time are compared in Figure 3. For the dimensionless luminosity $l \gtrsim 100$ ($\tau_T \gtrsim 10$) the cooling time becomes shorter than the Thomson time.

The author thanks Alan Lightman, Roland Svensson, and Greg Madejski for numerous discussions. Thanks are also due to Prof. J. Trümper for the hospitality at the Max-Planck-Institut für Extraterrestrische Physik, where the numerical computations presented here were performed. This work was supported in part by NASA grant NAGW-246.

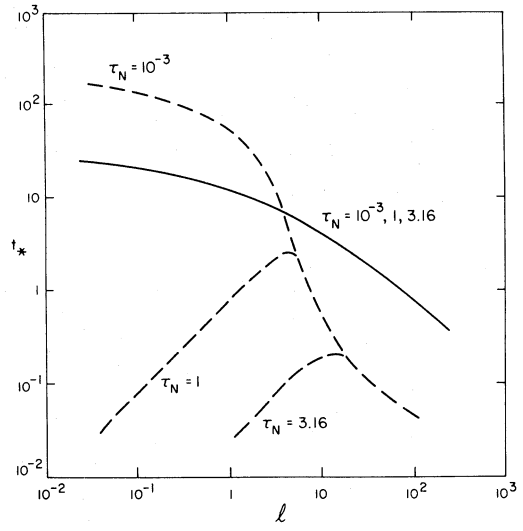


FIG. 3.—Cooling time $t_*^{\rm cool}$ (*solid curve*) and the *e-e* relaxation time $t_*^{ee}$ (*dashed curves*) in terms of the Thomson time $t_T \equiv [(n_+ + n_-)\sigma_T c]^{-1}$ as functions of the luminosity $l$ for three different $\tau_N$. In the shown luminosity region the $t_*^{\rm cool}$ is independent of $\tau_N$ within to a factor of $\sim 1.5$. For $t_*^{ee}$ the results of Stepney (1983*b*) have been used.

REFERENCES

Brown, R. W., Mikaelian, K. O., and Gould, R. J. 1973, *Ap. Letters*, **14**, 203.
Górecki, A., and Wilczewski, W. 1984, *Acta Astr.*, **34**, in press.
Gould, R. J. 1982, *Ap. J.*, **254**, 755.
Gould, R. J., and Schréder, G. P. 1967, *Phys. Rev.*, **155**, 1404.
Halpern, J. P. 1982, Ph.D. thesis, Harvard University.
Lightman, A. P. 1982, *Ap. J.*, **253**, 842.
Lightman, A. P., and Band, D. 1981, *Ap. J.*, **251**, 713.
Lorentz, M. 1981, *Max-Planck-Institut (MPE) Rept.*, No. 171.
Pozdnyakov, L. A., Sobol', I. M., and Sunyaev, R. A. 1977, *Soviet Astr.*, **54**, 1246.
Rothschild, R. E., Mushotzky, R. F., Baity, W. A., Gruber, D. E., Matteson, J. L., and Peterson, L. E. 1983, *Ap. J.*, **269**, 423.
Stepney, S. 1983*a*, in *Positron-Electron Pairs in Astrophysics*, ed. M. L. Burns, A. K. Harding, and R. Ramaty (New York: Am. Inst. Phys.), p. 373.
———. 1983*b*, *M.N.R.A.S.*, **202**, 467.
Stepney, S., and Guilbert, P. W. 1983, *M.N.R.A.S.*, **204**, 1269.
Sunyaev, R. A., and Titarchuk, L. G. 1980, *Astr. Ap.*, **86**, 121.
Svensson, R. 1982, *Ap. J.*, **258**, 335.
———. 1984, *M.N.R.A.S.*, in press.
Zdziarski, A. A. 1980, *Acta Astr.*, **30**, 371.
———. 1984, *Phys. Scripta*, **T7**, 124.

ANDRZEJ A. ZDZIARSKI: Harvard-Smithsonian Center for Astrophysics, 60 Garden Street, Cambridge, MA 02138